HYDROLOGICAL PROCESSES
Hydrol. Process. **22**, 2410–2423 (2008)
Published online 6 December 2007 in Wiley InterScience
(www.interscience.wiley.com) DOI: 10.1002/hyp.6833

Carbon isotope fractionation of dissolved inorganic carbon (DIC) due to outgassing of carbon dioxide from a headwater stream

Daniel H. Doctor,[1]*,† Carol Kendall,[1]† Stephen D. Sebestyen,[2] James B. Shanley,[3]† Nobuhito Ohte,[4] and Elizabeth W. Boyer[5]

[1] *US Geological Survey, 12201 Sunrise Valley Drive Reston, VA 20192*
[2] *State University of New York College of Environmental Science and Forestry, 1 Forestry Drive, Syracuse, NY 13210, US*
[3] *U.S. Geological Survey, 87 State St, Montpelier, VT 05602, US*
[4] *Division of Environmental Science and Technology, Kyoto University, Kyoto, 606-8502, Japan*
[5] *Dept. of Environmental Science, Policy and Management, 137 Mulford Hall, University of California, Berkeley, CA 94720, US*

Abstract:

The stable isotopic composition of dissolved inorganic carbon (δ^{13}C-DIC) was investigated as a potential tracer of streamflow generation processes at the Sleepers River Research Watershed, Vermont, USA. Downstream sampling showed δ^{13}C-DIC increased between 3–5‰ from the stream source to the outlet weir approximately 0·5 km downstream, concomitant with increasing pH and decreasing PCO_2. An increase in δ^{13}C-DIC of $2{\cdot}4 \pm 0{\cdot}1$‰ per log unit decrease of excess PCO_2 (stream PCO_2 normalized to atmospheric PCO_2) was observed from downstream transect data collected during snowmelt. Isotopic fractionation of DIC due to CO_2 outgassing rather than exchange with atmospheric CO_2 may be the primary cause of increased δ^{13}C-DIC values downstream when PCO_2 of surface freshwater exceeds twice the atmospheric CO_2 concentration. Although CO_2 outgassing caused a general increase in stream δ^{13}C-DIC values, points of localized groundwater seepage into the stream were identified by decreases in δ^{13}C-DIC and increases in DIC concentration of the stream water superimposed upon the general downstream trend. In addition, comparison between snowmelt, early spring and summer seasons showed that DIC is flushed from shallow groundwater flowpaths during snowmelt and is replaced by a greater proportion of DIC derived from soil CO_2 during the early spring growing season. Thus, in spite of effects from CO_2 outgassing, δ^{13}C of DIC can be a useful indicator of groundwater additions to headwater streams and a tracer of carbon dynamics in catchments. Copyright © 2007 John Wiley & Sons, Ltd.

KEY WORDS stable isotopes; carbon dioxide; DIC; headwater stream; catchment

Received 26 December 2006; Accepted 14 May 2007

INTRODUCTION

Processes that control carbon fluxes into and out of terrestrial ecosystems are currently receiving particular attention due to the role of the carbon cycle in providing positive feedbacks toward global climate change (e.g. Cox *et al*., 2000; Friedlingstein *et al*., 2001). Much work has focused on the transfer of CO_2 between the atmosphere, soils, and vegetation (Cramer *et al*., 2001); however, the links between hydrological processes and biogeochemical processes controlling CO_2 fluxes in these ecosystems remain ill-defined (Billett *et al*., 2004). Outgassing of CO_2 from surface waters is recognized as a significant component of the terrestrial carbon efflux (Kling *et al*., 1992; Hope *et al*., 2001; Richey *et al*., 2002; Billett *et al*., 2004). Other studies have shown CO_2 loss from surface waters occurs across a wide range of surface water environments (e.g. Kling *et al*., 1991; Pinol and Avila, 1992; Cole *et al*., 1994; Ohte *et al*., 1995; Jones and Mulholland, 1998; Cole and Caraco, 2001; Jones *et al*., 2003).

Nonetheless, relatively few studies have used stable isotopes of dissolved inorganic carbon (DIC) to specifically address the factors that control carbon fluxes in rivers (e.g. Taylor and Fox, 1996; Yang *et al*., 1996; Atekwana and Krishnamurthy, 1998; Amiotte-Suchet *et al*., 1999; Aucour *et al*., 1999; Karim and Veizer, 2000; Hélie *et al*., 2002; Mayorga *et al*., 2005), and fewer still in headwater catchment streams where potential for CO_2 loss is greatest (e.g. Kendall *et al*., 1992; Amiotte-Suchet *et al*., 1999; Palmer *et al*., 2001; Finlay, 2003).

In the present study, we present a high-resolution dataset of δ^{13}C values of DIC (δ^{13}C-DIC) collected from a small headwater forested watershed. The initial goal of the study was to use δ^{13}C-DIC as a tracer for quantifying soil water and groundwater contributions to streamflow. As we discovered, CO_2 outgassing greatly impacted the δ^{13}C values of stream DIC, thus complicating the use of this parameter as a tracer for streamflow generation studies while instead providing a tool for investigating CO_2 dynamics in streams.

* Correspondence to: Daniel H. Doctor, US Geological Survey, 12201 Sunrise Valley Drive Reston, VA 20192. E-mail: dhdoctor@usgs.gov
† The contributions of Daniel H. Doctor, Carol Kendall and James B. Shanley to this article were prepared as part of their official duties as United States Federal Government employees.

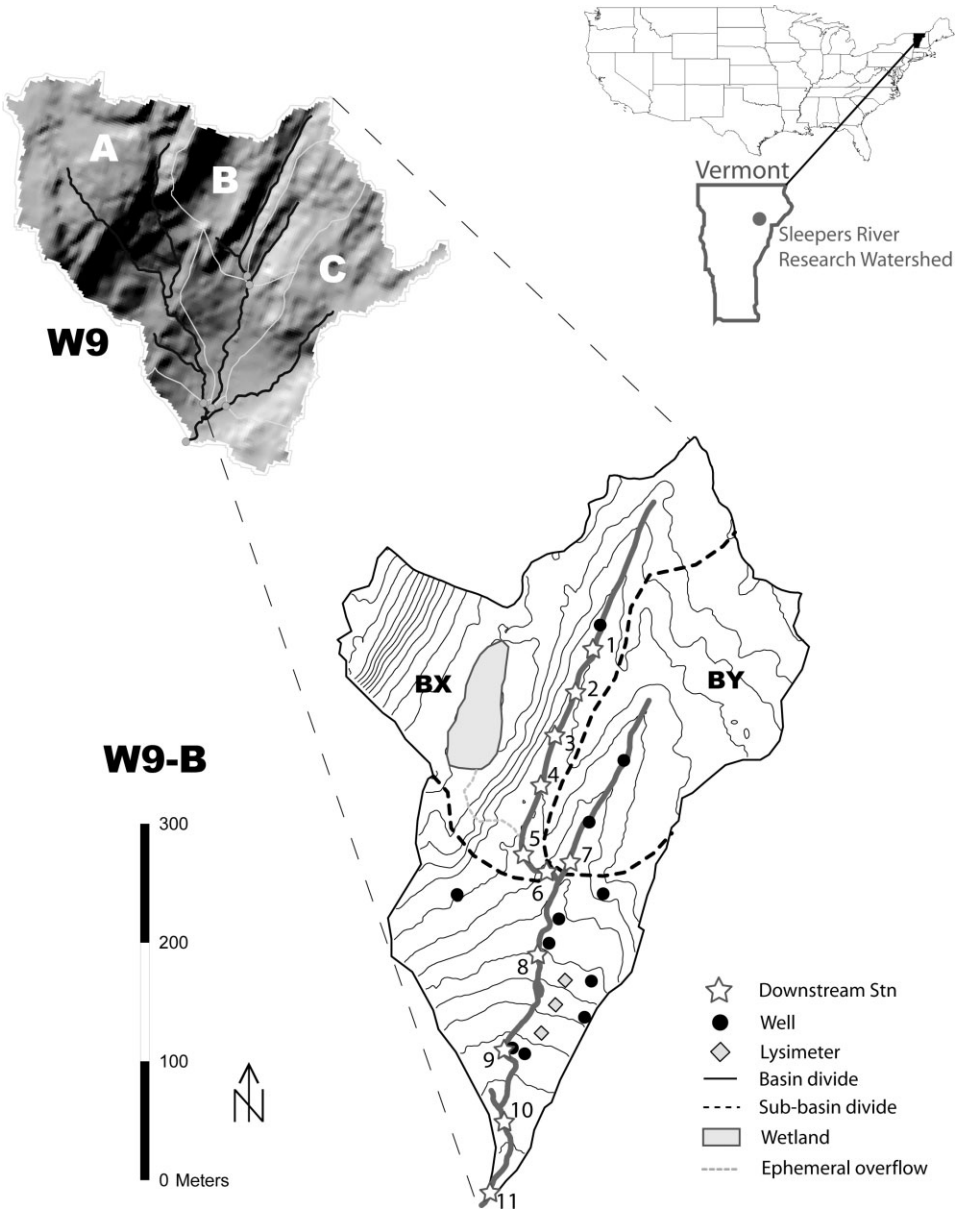

Figure 1. Study site location and map of the catchment W9 at Sleepers River, VT. The smaller catchment W9B is enlarged and its subcatchments BX and BY with locations of wells, lysimeters and downstream sampling points are indicated

STUDY SITE AND BACKGROUND

The Sleepers River Research Watershed is located in northeast Vermont, USA (http://nh.water.usgs.gov/projects/sleepers). The entire watershed consists of a series of nested catchments of varying area. This study was conducted in catchment W9 (an area of 41 ha) and its subcatchments (Figure 1). Catchment W9 is completely forested by northern hardwoods, dominated by sugar maple, yellow birch, white ash and American beech, with less than 5% conifers including balsam fir and red spruce.

The watershed lithology is predominantly metamorphic calcareous granofels interbedded with schist and shale with minor calcite (the Waits River Formation). The calcareous rich units contain approximately 50% calcite (minor dolomite) and they make up slightly less than half the formation (Hall, 1959). Overlying the bedrock is a mantle of dense basal till derived from the bedrock host which varies in thickness from 1–4 m (Shanley *et al*., 2003). The till is depleted of carbonate in the upper surface as a result of weathering but retains carbonate in its lower horizons (Kendall *et al*., 1999). Thus, the lower till and bedrock are the primary sources of stream and groundwater alkalinity in the catchment, the latter being as high as 20 mg C l^{-1} as DIC. On top of the till is an organic-rich soil of varying thickness locally classified as an inceptisol. This soil has numerous root casts and other enlarged preferential flow pathways permitting rapid stream response to recharge events (Hjerdt, 2002). Seepage into streams occurs predominantly along these preferential flow paths.

Dissolved organic carbon (DOC) has been shown to be a useful tracer of water flow paths through shallow soil horizons in this watershed (McGlynn *et al*., 1999; Hjerdt, 2002), and the stable oxygen isotopic composition

DOI: 10.1002/hyp

($\delta^{18}O$) of water has proved to be an effective tracer for quantifying sources of streamflow generation in this catchment (Shanley *et al.*, 2002a). Thus, DOC and $\delta^{18}O$ of water were measured in addition to DIC and $\delta^{13}C$-DIC as supplemental tracers of streamflow generation in this study.

The relation between groundwater levels and stream discharge during recharge events at the W9 subcatchment B was investigated in detail by Hjerdt (2002). Conclusions from this work were that (1) groundwater levels in wells in geomorphic depressions with shallow water tables responded more rapidly to recharge than wells on planar hillslopes; (2) the groundwater in the geomorphic depressions consistently displayed chemistry that was most similar to stream chemistry during recharge events; and (3) the stream in the uppermost portion of the catchment was fed primarily by shallow groundwater, which differed only slightly in chemical composition from the stream water composition measured in the lower portion of the catchment. The difference was attributed to the influence of direct precipitation, soil water and overland flow entering the stream downslope.

In a previous study at Sleepers River that utilized carbon isotopes for tracing stream flow generation, Bullen and Kendall (1998) identified two predominant flowpaths in the upper catchment surface that contribute to the stream chemistry: shallow flow through the carbonate-free soil zone (predominantly the organic horizon) with low $\delta^{13}C$, and deeper flow through less-weathered soil and till with higher $\delta^{13}C$. They concluded that the relative contributions of water from different flowpaths have a significant effect on stream $\delta^{13}C$-DIC, and that contributions of shallow unsaturated zone waters to stream flow during storm events increase with greater catchment soil thickness.

In light of these observations, one conceptual model for streamflow generation in this catchment is that shallow groundwater derived from geomorphic depressions in headwater reaches sets the stream chemistry at its origin, and changes in stream chemistry between the headwaters and catchment outlet are caused primarily by contributions of water from fast-flow pathways routed through riparian zones or via direct overland flow (McGlynn *et al.*, 1999; Shanley and Chalmers, 1999). The goal of this study was to test whether $\delta^{13}C$-DIC would be a useful tracer of soil water and groundwater to facilitate quantitative assessment of these contributions to streamflow.

SAMPLING AND ANALYTICAL METHODS

Water sampling began prior to the snowmelt events of 2003 and 2004 and continued throughout both snowmelt periods. Stream water samples were collected along reaches of flowing water. Groundwater samples were collected from single and nested wells located in a variety of hillslope and riparian environments across the subcatchment W9B (Figure 1). Depths of wells ranged from 2–4 m; all wells were screened at an interval of 1·74 m from the base upward. Soil water was sampled with zero-tension lysimeters at two locations (midslope and upslope) along the main hillslope in the W9B catchment. Depths of the lysimeters were 13, 43 and 140 cm for the midslope site and 10 and 46 cm at the upslope site. Groundwater and soil water samples were collected using a peristaltic pump; the wells and lysimeters were purged once to dryness and allowed to refill overnight prior to sampling. Measurements of pH and temperature were obtained in the field using a Mettler Toledo model MP120 pH meter($\pm$0·01 pH unit precision) and newly purchased probes (any use of trade, firm or product names is for descriptive purposes only and does not imply endorsement by the US Government). The meter was calibrated using pH 4·0 and pH 7·0 buffers each day prior to field use. Normal pH stabilization time when measuring samples in the field was 15–20 seconds.

Water samples for carbon isotope analysis of DIC were either collected manually or with an automatic water sampler. Samples obtained by autosampler (1 litre) were open to the atmosphere for up to 24 hrs before manual collection. Manually collected water was pulled into a 60 ml syringe and filtered through a binder-free 0·7 μm glass fibre syringe filter cartridge (Whatman Puradisc™ 25 GF/F) into 40 ml clear (for DIC) or amber (for DOC) pre-cleaned glass vials with septa caps. The vials for DOC were baked at 450 °C in a muffle furnace for at least 4 hours in order to remove traces of organic contaminants from the glass, and were triple rinsed with filtered samples in the field before filling. Syringe filters were flushed with 5–10 ml of sample water before filling all vials. The DIC sample vials were filled until a positive meniscus formed, then tightly capped so that no headspace or bubbles remained. The DOC samples were collected leaving approximately 1–2 ml of headspace. Both DIC and DOC samples were stored chilled between 0–5 °C until analysis, which took place within two months of sample collection.

Many authors have used $HgCl_2$ as a preservative for DIC carbon isotope samples in order to prevent biological activity in the sample; however, we elected not to use mercury due to the risk of compromising ongoing mercury studies in this watershed (e.g. Shanley *et al.*, 2002b). As an alternative, 5–10 mg of solid copper (II) sulphate pentahydrate (J.T. Baker Inc., analytical reagent grade) was added to each vial prior to sample collection. Winslow *et al.* (2001) demonstrated the efficacy of copper sulphate as an inhibitor of biological activity in comparison to several other preservatives, showing sample preservation with copper sulphate to be as good as that with mercuric chloride.

We conducted an independent holding-time test for DIC preservation on some stream samples treated with $HgCl_2$, $CuSO_4$, $CuCl_2$ and no preservative. The samples were collected among actively-growing filamentous algae along a reach of San Francisquito Creek in Palo Alto, CA. Six replicates of each treatment were collected; three were analysed the day after collection, and the other three were held chilled and in the dark for 9 months

DOI: 10.1002/hyp

before analysis. All samples were filtered through 0·2 μm polysulfone syringe filters. After storage, all samples exhibited an increase in δ^{13}C-DIC of approximately 0·25 per mil (on the order of the analytical error), except for those treated with $CuCl_2$ which exhibited precipitation of a copper carbonate phase and a decrease of approximately 0·5 per mil in δ^{13}C-DIC. There was no statistically significant difference between the samples preserved with $HgCl_2$ and $CuSO_4$; curiously, there was also no significant difference between the unpreserved samples and those preserved with $HgCl_2$ and $CuSO_4$. Our conclusion is that filtering through 0·2 micron filters is the best means to guard against fractionation of DIC by biological activity in stream samples. However, adding $CuSO_4$ as a preservative may provide an added degree of precaution. Isotopic analysis of $NaHCO_3$ standard solutions containing copper sulphate indicated that the copper sulphate had no effect upon the concentration nor isotopic composition of the DIC in solution outside of the precision of measurement (±0·2 mg C l^{-1} for DIC, and ±0·3‰ for δ^{13}C-DIC, $n > 30$). DIC and DOC samples were collected and analysed separately due to DIC samples being preserved with copper sulphate. DOC samples were filtered and stored chilled with no preservative added.

Concentrations and carbon isotopic composition of DIC and DOC were obtained using an OI Analytical 1010 TIC/TOC analyser interfaced with a GV IsoPrime™ continuous flow mass spectrometer according to a method modified after St Jean (2003). In this automated method, the sealed sample vials collected in the field are loaded directly into the autosampler of the TIC/TOC analyser. During analysis, a double-holed needle pierces the septa and a peristaltic pump pulls an aliquot of the sample from the base of the vial into a volumetric loop. As the liquid sample is pumped out of the vial, the headspace created in the vial is replaced with helium gas; however, a partial vacuum remains in the vial headspace. A flow of helium pushes the sample aliquot into a digestion chamber, whereupon 2 μl of 5% phosphoric acid is injected into the chamber. The chamber is heated to 90 °C and the sample is allowed to react for 2 min, after which the gas produced is purged out of the reaction vessel, dried through Nafion tubing and Drierite water trap and passed through the calibrated IR detector for CO_2 concentration measurement. The CO_2 pulse is then carried through a Hayasep Q® gas chromatography (GC) column for separation from other permanent gases, through a quartz tube containing 40 g cleaned native copper and 10 g silvered-cobalt heated to 65 °C, and finally through a magnesium perchlorate water trap before being introduced into the source of the mass spectrometer. For DOC analysis, a second step is performed whereby 10 μl of 100 g l^{-1} sodium persulphate solution is injected into the digestion chamber. The sample is heated to 100 °C and allowed to react for 6 min, during which time the DOC in the sample is oxidized to CO_2. This second pulse of gas is sparged from the reaction chamber, separated on the GC column, cleaned through the scrubber furnace and routed into the mass spectrometer. Additional details on the operation of the TIC/TOC analyser are provided in St Jean (2003).

Standard solutions of $NaHCO_3$ and potassium acid phthalate (KHP) were made using solids that had been analysed for their isotopic composition using an elemental analyser interfaced with a Micromass Optima™ mass spectrometer and calibrated against internal isotopic standards. The δ^{13}C values of the $NaHCO_3$ (J.T. Baker Inc., analytical reagent grade) and KHP (Mallinckrodt Inc., analytical reagent grade) solids were $-8{\cdot}0 \pm 0{\cdot}1$‰ ($n = 10$) and $-25{\cdot}0 \pm 0{\cdot}1$‰ ($n = 15$) respectively; these standards were used to correct the isotopic values obtained from the sample analyses for instrument drift and linearity and to normalize the δ^{13}C values to the Vienna Pee Dee Belemnite (VPDB) scale.

Solutions of KHP were made using de-ionized water obtained from a Milli-Q filtration unit that produces water with resistance in excess of 18 MOhms cm^{-1}. Solutions of $NaHCO_3$ were made using de-ionized water from the same filtration unit, and the water had been sparged with ultra-high purity He for at least 20 min to remove background CO_2. A stock solution of 1000 mg C l^{-1} was made using a weighed amount of $NaHCO_3$ or KHP that had been dried at 30 °C overnight and additional solutions of varying concentrations were made from volumetric dilutions of the stock. These standard solutions were then immediately poured off into vials and stored at room temperature before analysis. Standard solutions were discarded if not used within one month.

The TIC/TOC analyser reagents had organic carbon concentrations that ranged from 0·01–0·05 mg C l^{-1}, which is an order of magnitude lower than the precision of the carbon concentration measurements. DOC concentrations of lab and field blanks of de-ionized water filtered through the syringe filters revealed no contribution of DOC from the syringe, filter cartridges, nor the combusted sample vials ($0{\cdot}04 \pm 0{\cdot}01$ mg C l^{-1}, $n = 10$).

Unfiltered water samples for δ^{18}O of water analysis were collected in glass vials with Polyseal cone-lined caps. Analyses of δ^{18}O of water were performed on a Finnigan MAT 251 mass spectrometer by the CO_2 equilibration method (Epstein and Mayeda, 1953). Analytical precision (1σ) was less than ±0·05‰. Water δ^{18}O values were normalized and reported relative to the Vienna Standard Mean Ocean Water (VSMOW) scale.

Samples for cation and anion analyses were syringe-filtered using 0·45 μm membrane filters and the unacidified samples were kept chilled prior to analysis. Filters were flushed with 5–10 ml of sample prior to collecting sample. Bottles were Nalgene high-density polyethylene which had been triple soaked in de-ionized water prior to being brought into the field, and were triple-rinsed with filtered sample water before capping. Cations were analysed by ICP-OES at the State University of New York College of Environmental Science and Forestry, Syracuse, NY (SUNY-ESF). Anions were analysed by ion chromatography at SUNY-ESF.

DOI: 10.1002/hyp

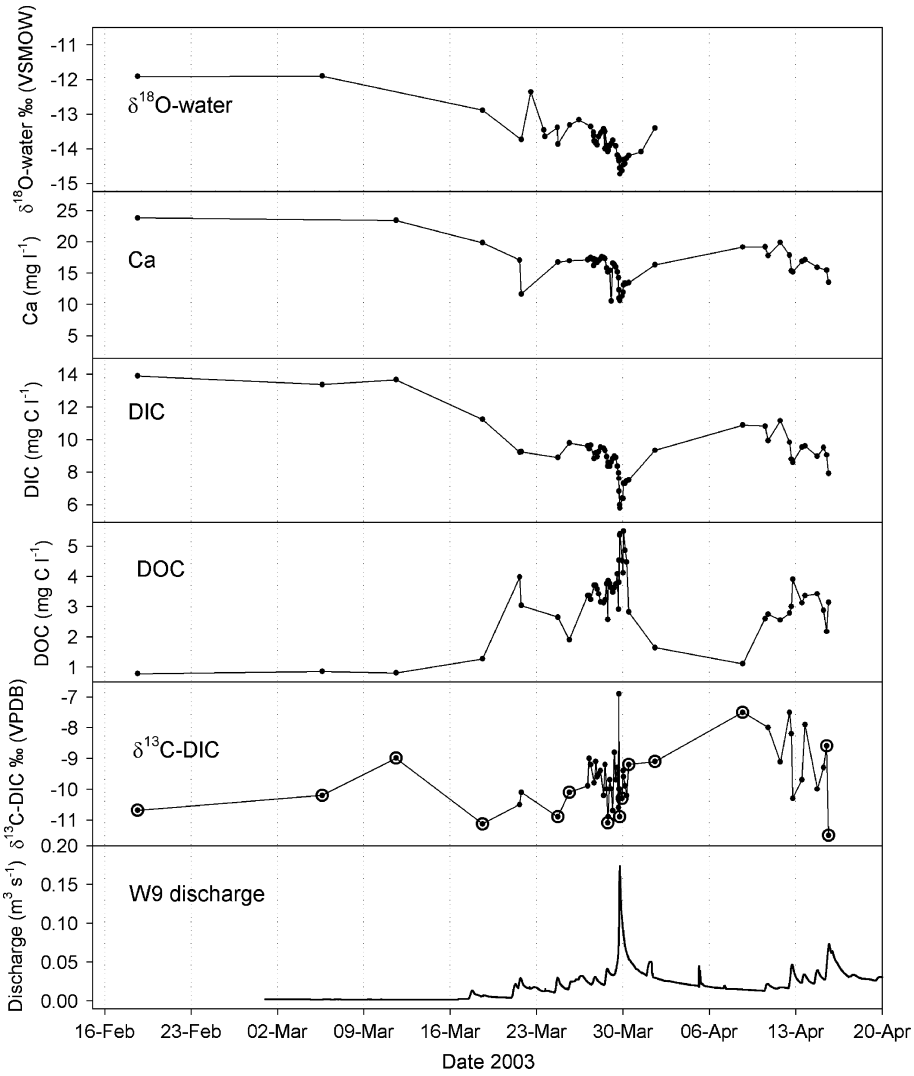

Figure 2. Data from the snowmelt period of 2003 for samples collected at the W9 weir. Circled points indicate manually-collected samples; all others were collected by autosampler

RESULTS

Snowmelt sampling of 2003 and 2004

The chemical and isotopic data collected during the snowmelt of 2003 are presented in time series in Figure 2 and the chemical and isotopic data collected during the snowmelt of 2004 are displayed in Figure 3. Snowmelt of 2003 began in late March, and occurred in two distinct phases. Most of the runoff occurred in the first phase, which exhibited a typical interval of diurnal melt pulses. Well hydrographs indicate that the onset of catchment-wide groundwater response to snowmelt began around March 18. The wells and lysimeters were all sampled on 24–25 March 2003 during a period of rising groundwater levels. As a result, the water sampled from wells and lysimeters likely represent mixtures of fresh snowmelt and water released from soil and shallow groundwater storage. A comparison of the chemical and isotopic compositions of stream water, groundwater and soil water shows that the water chemistry was generally similar between the snowmelt periods of 2003 and 2004 despite very different snowmelt progression. In 2003, a single large peak event dominated snowmelt while in 2004 snowmelt was prolonged and the peak discharges were relatively damped.

Variable mixing between soil water and groundwater end-members in the stream water is evident in a plot of δ^{18}O versus DIC concentration for stream water samples collected at the W9 weir during snowmelt of 2003 and 2004 (Figure 4a). However, δ^{18}O of water is a conservative parameter while the δ^{13}C-DIC is not. When δ^{18}O of water is plotted against δ^{13}C-DIC, the stream water samples do not plot between the soil water and groundwater fields as would be expected (Figure 4b). The stream water samples have δ^{13}C-DIC values higher than both soil water and groundwater end-members, indicating non-conservative behaviour in the carbon isotopes of DIC. To investigate the causes of the apparent non-conservative behaviour of δ^{13}C-DIC, we sampled along downstream transects in addition to the weirs during snowmelt of the following year (2004).

Two downstream sampling transects were conducted in the headwaters of subwatershed B in April of 2004, from the initial stream seep in BX to the subcatchment

DOI: 10.1002/hyp

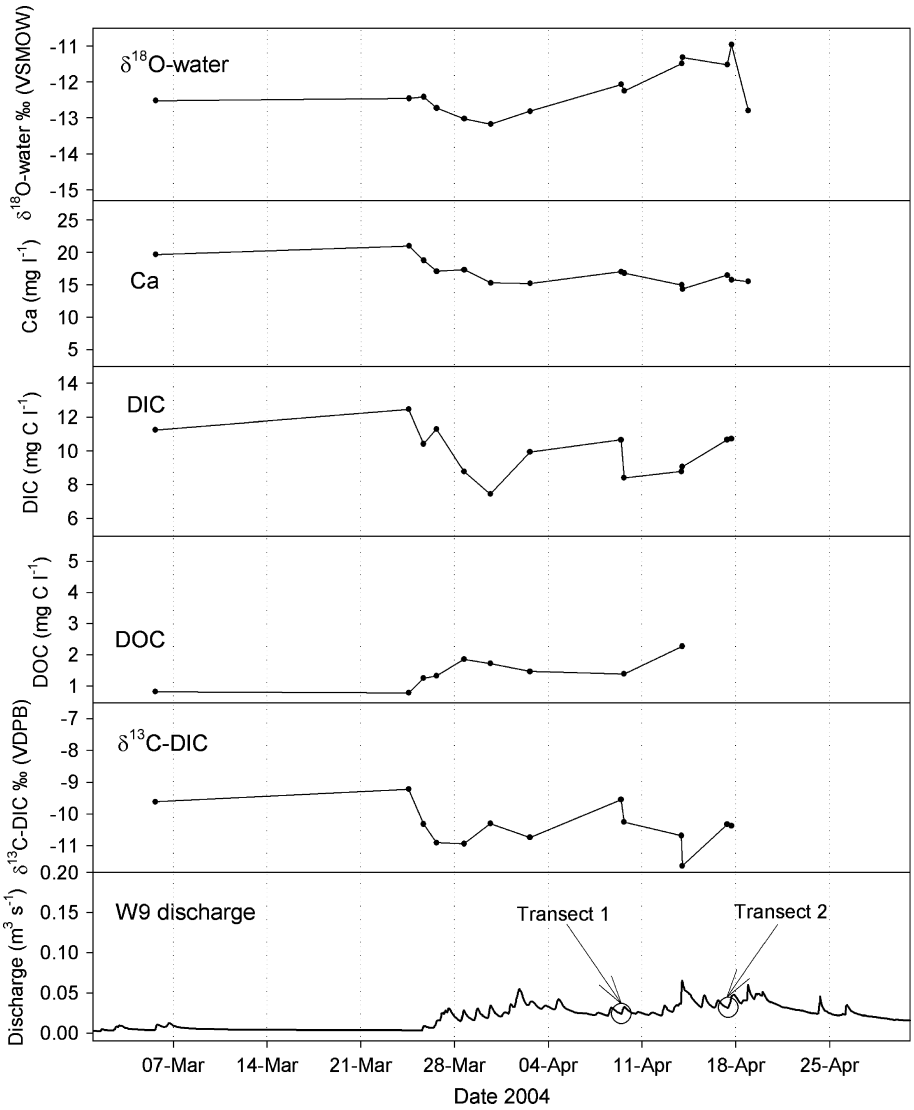

Figure 3. Data from the snowmelt period of 2004 for samples collected at the W9 weir. Chemical and isotopic data show similar ranges and variability with discharge as during the 2003 snowmelt period, although more damped. Arrows indicate the time of downstream transect sampling along stream W9BX

weir W9B (sampling locations are shown in Figure 1). Downstream transect samples were collected on 9 April and 17 April 2004; samples were collected after an initial snowmelt pulse had passed, but before and after the peak snowmelt discharge. Discharge was slightly greater during the second transect sampling (Figure 3). As with the data from the catchment outlet weir W9 (Figure 4), the transect data fall between values of local shallow groundwater in a plot of DIC versus $\delta^{18}O$ (Figure 5a); however, the $\delta^{13}C$-DIC values of the stream water again lie above a theoretical mixing line between these groundwaters on a plot of $\delta^{13}C$-DIC versus $\delta^{18}O$ (Figure 5b).

Measurement of pH in 2004 allowed for the estimation of PCO_2 of the water samples to be calculated according to the relationship:

$$\frac{C_T \alpha_0}{K_H} = PCO_2 \quad (1)$$

where C_T is the total DIC concentration (mol C l^{-1}) in the sample, α_0 is the ionization fraction between CO_2 and H_2CO_3 (Stumm and Morgan, 1981) and K_H is the Henry's Law equilibrium constant for CO_2 in water. Since K_H is temperature-dependent, its value was estimated from the temperature of the sample at the time of collection using the relationships given in Telmer and Veizer (1999).

Excess PCO_2 ($ePCO_2$) is the ratio of the PCO_2 in the sample calculated from field-determined pH and temperature to that of the atmosphere (Neal, 1988). The $ePCO_2$ value is thus a multiplicative factor of the atmospheric concentration; a value of $ePCO_2$ of 20 indicates the water sample has a PCO_2 20 times higher than that of the atmosphere. The greatest source of error in the calculation of $ePCO_2$ is the pH measurement. Based upon a pH measurement error of $\pm 0{\cdot}02$ pH units, the error on the calculated $ePCO_2$ values is 8% or less. The atmospheric value of CO_2 concentration used for the calculation was 378 ppmV.

DOI: 10.1002/hyp

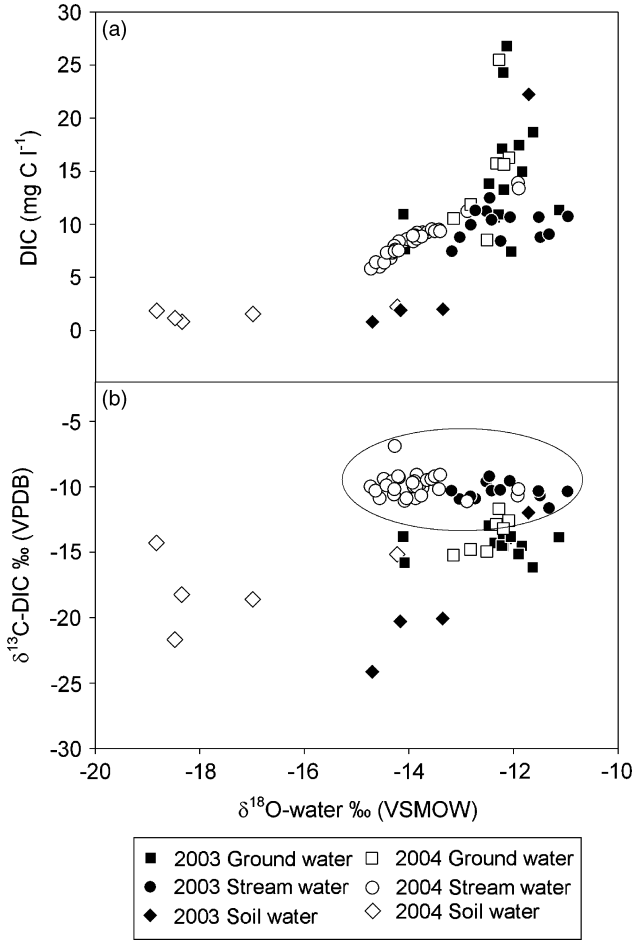

Figure 4. $\delta^{18}O$ of water, DIC, and $\delta^{13}C$-DIC for samples collected during snowmelt at the W9 weir in 2003 and 2004: (a) $\delta^{18}O$ of water versus DIC concentration and (b) $\delta^{18}O$ of water versus $\delta^{13}C$-DIC. Data encircled in (b) illustrate departure from the mixing trend observed in (a)

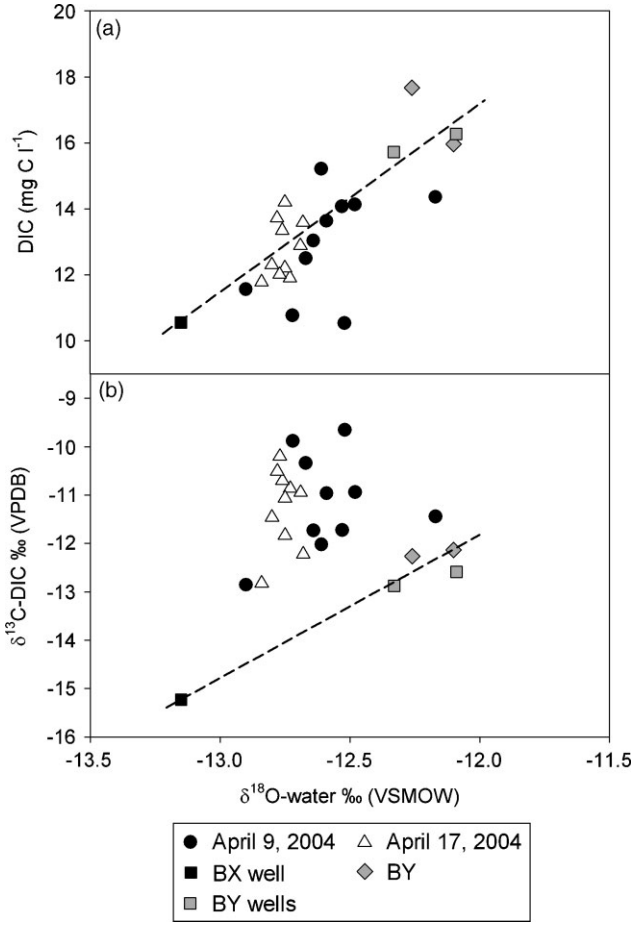

Figure 5. $\delta^{18}O$ of water, DIC and $\delta^{13}C$-DIC for downstream transect samples collected in 2004: (a) $\delta^{18}O$ of water versus DIC concentration and (b) $\delta^{18}O$ of water versus $\delta^{13}C$-DIC

All water samples for which PCO_2 could be calculated exhibited excess PCO_2. The ePCO_2 values of groundwater collected in 2004 were variable, ranging from 4–74 with a mean of 24·5. However, the ePCO_2 values of groundwater in hollows immediately above the stream origins in BX and BY were nearly identical, at 22 and 21 respectively. In spite of the high variability in DIC concentrations and ePCO_2 values, the $\delta^{13}C$-DIC values of the groundwater were relatively consistent, with a mean value of $-13{\cdot}4 \pm 1{\cdot}4‰$ ($n = 8$). Lysimeter soil water exhibited lower average DIC (1·6 mg C l^{-1}), ePCO_2 (4·8), and $\delta^{13}C$-DIC ($-21{\cdot}5 \pm 2{\cdot}3‰$, $n = 3$) than groundwater. Stream water collected at the W9 weir in 2004 exhibited ePCO_2 values ranging from 1·3–8·2.

A steady increase in pH with downstream distance was observed for both transects, except for a decrease in pH at 180 m downstream where an ephemeral tributary seep enters the stream (Figure 6). The $\delta^{13}C$-DIC values from both sets of transect samples also show a general increase downstream, and the values were remarkably similar in both sampling periods.

Higher Ca^{2+} concentrations correspond to higher DIC concentrations in the groundwater within the immediate vicinity of the stream, indicating that carbonate weathering is a primary source of DIC (Figure 7a). Although the stream transect samples do not exhibit a strong trend in Ca^{2+}, the data suggest an overall downstream increase resulting from mixing between sources similar to the BX and BY well waters. There was no evidence of calcium carbonate precipitation due to CO_2 loss that would have resulted in a downstream decrease in Ca^{2+} concentration; the stream water was calculated to be below calcite saturation at all times.

Higher DIC concentrations in the transect samples correspond to lower $\delta^{13}C$-DIC values (Figure 7b). However, two sample locations are of note: one taken from the well immediately above the stream, and the other taken from the seep at the stream origin. These two samples do not exhibit ^{13}C enrichment of DIC from CO_2 outgassing as they were collected from a source that was still in contact with soil CO_2. Thus, these samples fall outside the downstream transect trend of increasing $\delta^{13}C$-DIC with DIC loss, and instead may define a trend of more conservative mixing in the subsurface.

For both 2004 downstream transects, $\delta^{13}C$-DIC increased as ePCO_2 decreased (Figure 8a). The downstream transect samples collected during lower flow on 9

DOI: 10.1002/hyp

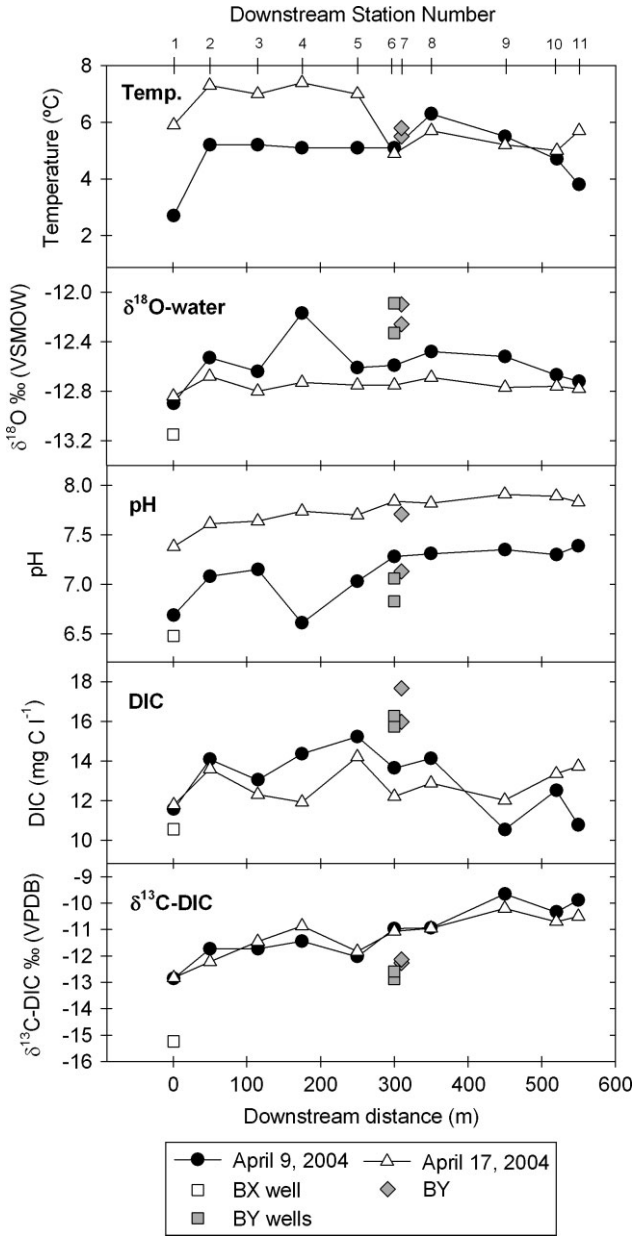

Figure 6. Downstream transects collected during snowmelt in April 2004 from subwatershed B. Numbers at the top of the graph are the site numbers from Figure 1

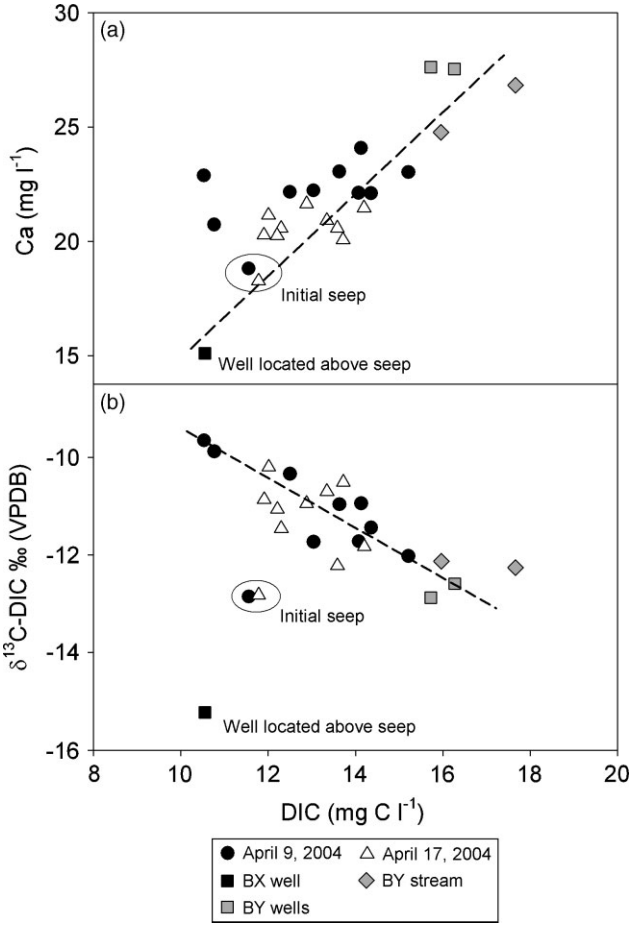

Figure 7. DIC concentration plotted against (a) calcium concentration and (b) δ^{13}C-DIC for downstream transect samples

April (transect 1) exhibited higher ePCO_2 than the samples taken on 17 April (transect 2) when flow was slightly greater. The downstream relation between δ^{13}C-DIC and ePCO_2 is approximated by an exponential decay function. Plotting δ^{13}C-DIC against the natural log of ePCO_2, an ordinary least squares linear regression reveals strong correlations for both transect 1 ($r^2 = 0{\cdot}96$) and transect 2 ($r^2 = 0{\cdot}90$); the slope of each regression line is nearly identical between each set of transect data (Figure 8b). According to those slopes, the increase in δ^{13}C-DIC per log unit decrease of ePCO_2 for transects 1 and 2 were 2·3‰ and 2·4‰, respectively.

Seasonal trends

Downstream transects were also sampled in June and July, 2003. Downstream increases in δ^{13}C-DIC were greater and more rapid in the summer months than during the snowmelt periods (Figure 9). The transect samples collected in June and July showed an increase in δ^{13}C-DIC of 3‰ within the first 20 m of stream flow, while in the snowmelt period a 3‰ increase in δ^{13}C-DIC took place over a distance of 450 m. The stream samples collected in June were consistently higher in δ^{13}C-DIC than the stream samples collected in July, although the July samples had greater DIC concentrations.

DIC concentrations in stream samples collected in early and mid-summer (June and July) are lower than those collected during snowmelt (April), while δ^{13}C-DIC span similar ranges (Figure 10). The seep at the BX stream origin consistently shows the lowest δ^{13}C-DIC of the stream transect samples; the stream samples collected in June show the highest δ^{13}C-DIC values.

DISCUSSION

Sources of DIC to catchment waters

The rationale for using the carbon isotope value of DIC as a tracer of stream-flow processes stems from the large δ^{13}C difference generally observed between soil waters which obtain most of their DIC from respired soil CO_2, and groundwater which obtains DIC from a mixture of soil CO_2 and carbonate minerals (Deines *et al.*, 1974).

DOI: 10.1002/hyp

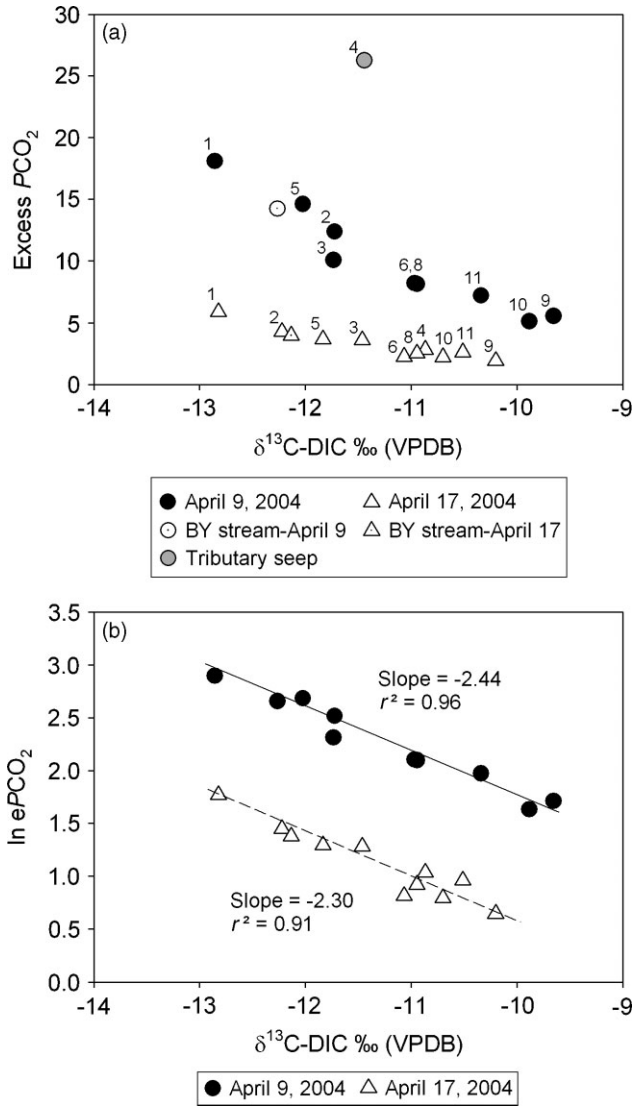

Figure 8. (a) δ^{13}C-DIC plotted with excess PCO_2 for both sets of transect samples. Symbol sizes encompass the estimated error of the values plotted. Numbers indicate sampling station (see Figure 1); station 4 from transect 1 is near to a tributary seep and showed high excess PCO_2. (b) An exponential relationship exists between the δ^{13}C-DIC and excess PCO_2. When plotted as δ^{13}C-DIC versus ln($ePCO_2$), the slopes of the two sets of transect data are nearly identical and indicate an increase in δ^{13}C-DIC of roughly 2·4‰ per natural log unit decrease in $ePCO_2$

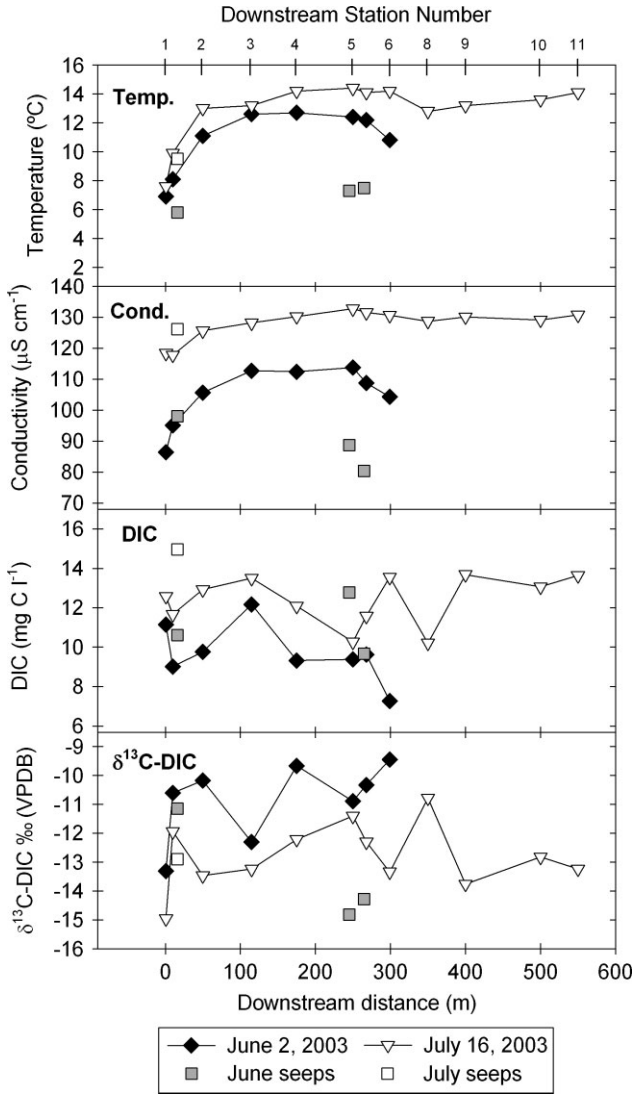

Figure 9. June and July downstream transect sampling in BX. Downstream variability in DIC and δ^{13}C-DIC at stations 1, 3 and 5 is related to discrete zones of shallow groundwater seepage observed entering the stream channel along preferential flowpaths

Due to this difference (often of the order 10‰), the δ^{13}C of DIC can discriminate between soil water and groundwater contributions to streamflow during recharge events (Kendall *et al*., 1992). At Sleepers River, concentrations of DIC in groundwater are consistently the highest measured in the catchment, while DIC concentrations in soil waters are lower. Thus, the DIC concentration itself is a relatively good indicator of variable contributions from soil water and groundwater in this catchment, as is Ca^{2+} concentration.

A pattern of decreased concentrations of DIC in stream water during the peak snowmelt returning to higher concentrations during flow recession indicates that contributions of water derived from shallow flowpaths through the soil and riparian zones increase as stream discharge increases; this interpretation is supported by the increases in DOC concentrations with increased runoff (Figure 2 and Figure 3). Peaks in DOC concentration were consistent with peaks in stream discharge throughout both snowmelt periods.

Carbonate dissolution is a primary source of Ca^{2+} and DIC to the groundwater of this catchment. Carbonate dissolution mainly occurs in groundwater within the lower till (Bullen and Kendall, 1998) by reaction with weak carbonic acid resulting from soil CO_2 in solution, whereby half of the DIC in solution (as HCO_3^-) is derived from the calcium carbonate and half from the soil CO_2. In an open system, the PCO_2 of the soil will establish equilibrium with the solution and the fraction of DIC derived from soil CO_2 will generally be greater than 50%. As a result, there is an excess of CO_2 in the well waters compared to that which would be expected solely due to carbonic acid weathering of carbonate at chemical equilibrium, evidenced by elevated ePCO_2 and low δ^{13}C of DIC values in groundwater.

DOI: 10.1002/hyp

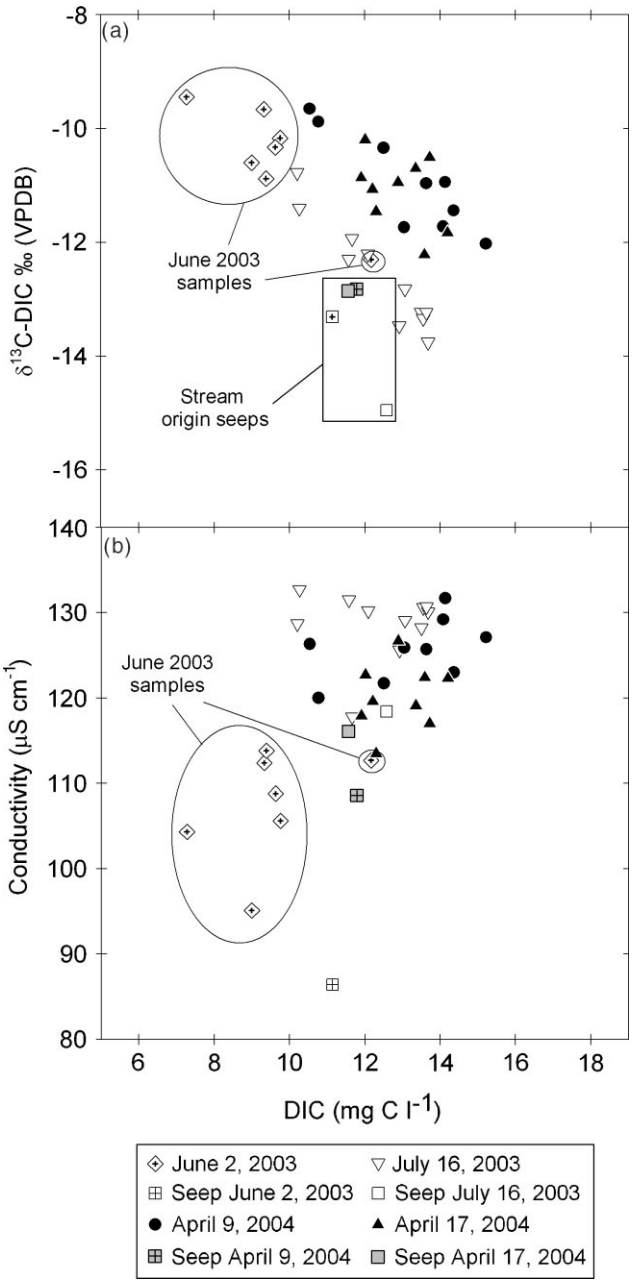

Figure 10. (a) April samples have higher DIC than June and July samples, yet a similar range in δ^{13}C-DIC values. The seep at the stream origin consistently has lower δ^{13}C-DIC values than the stream in all seasons. (b) The June samples show the lowest DIC and conductivity of the stream waters and the highest δ^{13}C-DIC values, resulting from rapid outgassing of CO_2 at the stream source and at other discrete groundwater inputs (see Figure 9). Samples collected in mid-July show the lowest measured δ^{13}C-DIC values of the stream

Carbon isotope composition of soil water and groundwater DIC

The carbon isotope evolution of DIC in water depends upon whether the water is an open or closed system with respect to soil CO_2 (Deines *et al*., 1974). Under theoretical open-system conditions, the fluid maintains chemical and isotopic equilibrium with an infinite reservoir of soil gas, whereas under closed-system conditions the fluid is removed from contact with this infinite gas reservoir at some point during its chemical evolution. Both conditions assume water residence times are long enough to achieve significant isotopic exchange, which generally holds true in groundwater due to fast reaction kinetics in the carbonate system relative to residence times (Deines *et al*., 1974). If the water is in contact with carbonate minerals such as calcite, then dissolution of the carbonate takes place. Continued isotopic exchange with soil CO_2 under open system conditions will drive the δ^{13}C values of DIC toward the more negative values of soil CO_2. Therefore, δ^{13}C values of DIC in soil and groundwater generally reflect a mixture of carbonate mineral dissolution and soil CO_2.

Soil CO_2 results from the heterotrophic oxidation of soil organic matter as well as from respiration from plant roots. Both of these processes occur with negligible isotopic discrimination between the organic matter substrate and the CO_2 produced (Park and Epstein, 1961; Lin and Ehleringer, 1997). Thus, δ^{13}C of CO_2 produced by respiration in the soil will be approximately equivalent to δ^{13}C of the predominant organic matter. The Sleepers River Watershed is dominated by C3 vegetation, and the isotopic composition of the soil organic matter falls in the range $-23‰$ to $-30‰$ with an average value of $-27‰$. Measurements of soil CO_2 made in the summer of 1991 show δ^{13}C of soil CO_2 was $-21{\cdot}4‰$ at a depth of 30 cm and $-22{\cdot}2‰$ at a depth of 120 cm (unpublished USGS data). These values reflect the dominant C3 vegetation in the watershed, with some ^{13}C enrichment.

Several processes can potentially increase the δ^{13}C value of the soil CO_2: (1) exchange with atmospheric CO_2; (2) diffusion of CO_2 out of the soil; or (3) ^{13}C enrichment of the organic matter source due to decomposition. Exchange with atmospheric CO_2 will enrich the bulk soil CO_2 in ^{13}C, since the δ^{13}C value of atmospheric CO_2 is approximately $-8‰$. Diffusion of CO_2 through the soil surface may also result in fractionation on the order of $+4{\cdot}4‰$ (Cerling *et al*., 1991; Amundson *et al*., 1998). This process, however, is dependent upon the rate of soil respiration and the concentration gradient of CO_2 within the soil, which in winter months is lower than in summer (Rightmire, 1978; Davidson, 1995). Another possibility is that the soil organic matter source for respired CO_2 has itself been enriched in ^{13}C due to decomposition at depth (Davidson, 1995; Poage and Feng, 2004). At Sleepers River, the ^{13}C enrichment of the soil CO_2 is minor and does not preclude the use of the δ^{13}C of soil CO_2 as a means of distinguishing between carbon sources to DIC in this system.

The δ^{13}C value of a native calcite sample from the Sleepers River watershed was determined to be $-2‰$ (Bullen and Kendall, 1998). Taking the δ^{13}C of soil CO_2 to be $-22‰$, DIC in groundwater produced solely through carbonic acid weathering of calcite should have a δ^{13}C-DIC of $-12‰$ at equilibrium, obtaining half of the DIC from calcite and half from dissolved CO_2. However, most of the groundwater sampled across the watershed exhibits δ^{13}C-DIC values of $-13{\cdot}0‰$ or lower. Based upon the measured δ^{13}C-DIC isotopic compositions of the groundwater in 2003, the average calculated soil CO_2

DOI: 10.1002/hyp

contribution to groundwater DIC in this catchment is greater than 60%. Thus, δ^{13}C-DIC values of well waters reflect an excess of CO_2 from the soil as expected.

Downstream transects

We observe strong, rapid increases in δ^{13}C-DIC between the point of initial seepage into the stream and short distances downstream. Our interpretation that downstream increases in δ^{13}C-DIC are due to outgassing of CO_2 is based upon several lines of evidence. First, the calculated ePCO_2 steadily decreases with distance downstream, indicating that CO_2 evasion is occurring (Figure 8). DIC in subsurface waters that flow into streams is not in chemical and isotopic equilibrium with the atmosphere because CO_2 concentrations in the soil zone can be 20–100 times higher than the atmospheric concentration (Cosby *et al*., 1985). In this study, the shallow groundwater in hollows immediately upstream of the BX stream source during the 2004 snowmelt had ePCO_2 values of approximately 20. As a result, CO_2 is lost to the atmosphere as this shallow groundwater seeps into the open channel. Other studies have documented shifts of δ^{13}C-DIC of up to 5‰ as a result of CO_2 outgassing at carbonate springs (Michaelis *et al*., 1985) and in acidic headwater catchments (Palmer *et al*., 2001).

Dissolution of carbonate minerals might also result in increases in δ^{13}C-DIC with corresponding increases in Ca^{2+} concentrations. However, we observe an inverse relation between Ca^{2+} concentrations and δ^{13}C-DIC in our downstream transect samples (Figure 7). Localized decreases in δ^{13}C-DIC with increasing DIC and Ca^{2+} concentrations is evidence of rising groundwater entering the stream along shallow flow paths, contributing a source of DIC to the stream that has a δ^{13}C signature more negative than the stream water itself. In spite of these groundwater inputs, the δ^{13}C-DIC of the stream water continues to become more positive with decreasing ePCO_2 (Figure 8).

In order to test for mixing of waters with elevated δ^{13}C values accounting for the downstream increase in δ^{13}C-DIC, we compared the mixing relation between δ^{18}O and DIC to that between δ^{18}O and δ^{13}C-DIC of the transect samples. We find a linear mixing relation between δ^{18}O and DIC, indicating soil water and shallow groundwater from hollows as the end members (Figure 5a). However, the δ^{13}C-DIC values all fall above the mixing line (Figure 5b). This indicates that mixing between waters is not the cause of the elevated δ^{13}C values, and lends further support to the hypothesis that CO_2 outgassing results in increases in the δ^{13}C-DIC.

Seasonal trends and flushing of DIC

Two transects taken along the same stream reach in the spring and summer months of 2003 also exhibit downstream ^{13}C enrichment of DIC (Figure 9). In comparison with the winter sampling, the spring and summer sampling shows that the increase in δ^{13}C-DIC is more rapid and pronounced close to the stream source. For example, in July 2003 an increase in δ^{13}C-DIC of nearly 4‰ occurred within the first 20 m of stream flow, whereas an increase of only 1‰ was observed over a similar distance in the snowmelt period of 2004. This is likely the result of the greater production of soil CO_2 during the warm growing season that results in a higher PCO_2 contrast between the soil zone and the atmosphere. Thus, CO_2 outgassing from the stream is expected to be more pronounced in the warmer months than during the colder months.

The greater production of soil CO_2 also results in more negative δ^{13}C-DIC values of the shallow groundwater at the stream origin. However, it is interesting to note that δ^{13}C-DIC values of the samples collected further downstream in the early summer (June) were the highest measured among the transects (Figure 10). In addition to DIC, the conductivity values of the June samples were the lowest of any measured, indicating that much of the ionic species associated with groundwater had been flushed from the flow paths supplying water to the stream. The more dilute waters at the start of the growing season would then acquire DIC primarily from soil CO_2, rather than from groundwater, resulting in the very low δ^{13}C-DIC value measured at the seep (2‰ lower than the seep values measured in April or July). Although we lack the pH data necessary to determine the PCO_2 of the June and July samples, we hypothesize that a greater proportion of the DIC in the June samples would have been in the form of CO_2 than in the July or snowmelt samples. When this water seeped out into the stream channel, it would thus have experienced the most pronounced CO_2 outgassing, and resulted in the highest δ^{13}C-DIC values we observe.

Effect of CO_2 outgassing on δ^{13}C-DIC

CO_2 will diffuse out of waters when the PCO_2 of the solution is greater than that of the ambient atmosphere. As CO_2 is lost, there is a concomitant shift in the isotopic composition of the DIC remaining in solution. Zhang *et al*. (1995) reported minimal (1‰) kinetic isotopic fractionation during outgassing of CO_2 from water; Usdowski and Hoefs (1990) reported a similar result for the kinetic absorption of CO_2 by water. These studies were conducted in closed systems under low pH conditions (<4) such that the majority of the DIC species were as dissolved CO_2. However, Marlier and O'Leary (1984) determined the kinetic carbon isotope fractionation factor for the dehydration of bicarbonate ($HCO_3^- \rightarrow CO_2$) to be $\alpha = 1{\cdot}0147$ in an open system experiment. The per mil fractionation ε, as defined by

$$\varepsilon = (\alpha - 1) \times 1000 \quad (2)$$

is therefore $\varepsilon_{HCO3^- - CO2} = 14{\cdot}7‰$ at 24 °C. This is approximately 7‰ greater than the equilibrium value of $\varepsilon_{HCO3^- - CO2} = 8‰$ reported by several others (Mook *et al*., 1974; Zhang *et al*., 1995; Szaran, 1997). Moreover, Herczeg and Fairbanks (1987) observed a similar magnitude of carbon isotope fractionation (−13‰) during absorption of atmospheric CO_2 by highly photosynthetic

DOI: 10.1002/hyp

lake water at pH = 9·5. Thus, under open-system conditions favourable for the rapid exchange of CO_2 at pH 6·5–8 (where HCO_3^- is the dominant carbonate species), the change in δ^{13}C-DIC due to the dynamic exchange of CO_2 between gas and water is greater than that expected at chemical and isotopic equilibrium.

Hendy (1971) describes in detail the geochemical reactions and accompanying isotopic fractionation during CO_2 outgassing and concomitant calcium carbonate precipitation. Michaelis *et al*. (1985) concluded that this process is best described by a kinetic model rather than by Rayleigh-type fractionation. Although the precipitation of calcium carbonate is not detected in the stream studied here, the works of Hendy (1971) and Michaelis *et al*. (1985) are still relevant because the strong carbon isotope fractionation between dissolved CO_2 and HCO_3^- occurs independent of carbonate mineral precipitation. The kinetics of this process are controlled by: (1) the diffusion of CO_2 through the upper surface layer at the water/air interface; and (2) conversion of HCO_3^- to CO_2 as the loss of CO_2 is compensated through the ionic balance of the carbonate species. These two processes are dependent upon temperature, pH, the PCO_2 gradient between the water and the atmosphere with which it is in contact, and turbulence of flow.

Hendy (1971) concluded that isotopic fractionation of HCO_3^- due to CO_2 loss becomes significant when the PCO_2 of the solution is greater than twice that of the surrounding atmosphere. In our study, we found that δ^{13}C-DIC values increased ~3‰ with decreasing PCO_2 from an initial ePCO_2 of 5·9 down to ePCO_2 of 1·9 (Figures 8a, 17 April transect). Since the PCO_2 of the soil zone is often much greater than twice the PCO_2 of the atmosphere, an increase in δ^{13}C-DIC due to CO_2 outgassing is likely to occur in the majority of settings where water exits the subsurface and flows into the open atmosphere.

Alternative interpretations of increasing downstream δ^{13}C-DIC values

Several authors have postulated that carbon isotope exchange with atmospheric CO_2 ($\delta^{13}C \sim -8‰$) is partly responsible for the increasing downstream δ^{13}C-DIC values that they have measured in stream and river waters (e.g. Taylor and Fox, 1996; Yang *et al*., 1996; Atekwana and Krishnamurthy, 1998; Amiotte-Suchet *et al*., 1999; Aucour *et al*., 1999; Karim and Veizer, 2000; Hélie *et al*., 2002; Mayorga *et al*., 2005). However, in areas where CO_2 outgassing occurs, *isotopic* equilibrium between dissolved CO_2 and atmospheric CO_2 can only be attained after *chemical* equilibrium has been achieved. Thus, if a chemical drive for CO_2 evasion exists, the isotopic composition of the DIC will be primarily affected by the outgassing of CO_2 rather than by carbon isotope exchange accompanying CO_2 invasion from the atmosphere.

A second common interpretation of a downstream increase in δ^{13}C-DIC values is that DIC uptake through growth by aquatic plants enriches the remaining DIC in ^{13}C (e.g. Hellings *et al*., 2001). This effect is certainly probable where aquatic photosynthesis is high. However, in the stream we studied at Sleepers River this is an unlikely interpretation, as we did not observe evidence of high aquatic photosynthesis. Since the stream was cold during snowmelt (<8 °C) and was light-limited and low in nutrients during June and July, in-stream photosynthesis is not likely to have exerted a strong influence over the DIC in this headwater catchment setting. Moreover, the greatest δ^{13}C-DIC increases we observed occurred within the first 10–20 m of flowing reaches (in the absence of pools or large riffles), or immediately downstream of a point of groundwater influx, thus supporting our interpretation of CO_2 outgassing.

CONCLUSIONS

The stable isotopic composition of dissolved inorganic carbon (δ^{13}C-DIC) was studied as a potential tracer of streamflow generation processes during snowmelt at the Sleepers River Research Watershed, VT. We measured δ^{13}C-DIC in order to distinguish between soil water and groundwater end-members in stream water samples; however, the δ^{13}C-DIC of stream water did not fall along a mixing line between the soil water and groundwater compositions. In all of the stream water samples, the δ^{13}C-DIC compositions were more positive than would be expected from mixing alone. The explanation for this 're-setting' of the stream water δ^{13}C-DIC from the point of seepage is that outgassing of CO_2 causes an increase in δ^{13}C-DIC. Evidence for this exists at the origin of the stream (BX), where the emerging groundwater exhibits a positive shift in δ^{13}C-DIC ranging between 1 and 4‰ over a distance of a few tens of metres. In the summer months, the effect is enhanced due to probable higher PCO_2 contrast between the soil and the atmosphere that would result in a more rapid and pronounced increase in δ^{13}C-DIC downstream.

In spite of the CO_2 outgassing effect on δ^{13}C of DIC, discrete areas of shallow groundwater seepage entering the stream channel are identifiable by decreases in the δ^{13}C-DIC of the stream water and corresponding increases in DIC concentration during snowmelt. Thus, δ^{13}C-DIC of stream water can be used as an indicator of zones of groundwater inputs in headwater streams where high PCO_2 contrast exists between the groundwater and stream water, and perhaps in larger streams and rivers as well. Moreover, we show that contributions of soil CO_2 to stream DIC vary under changing seasonal flow conditions, and we hypothesize that snowmelt events flush DIC from flowpaths to streams such that more dilute post-melt waters in the early growing season carry a greater proportion of their DIC as soil CO_2. Seasonal variability in soil zone PCO_2 will have an effect on the δ^{13}C-DIC of stream water that will be overprinted by the increasing δ^{13}C values due to outgassing, but is nonetheless an observable trend.

We have found that the isotopic composition of DIC in streams may be rapidly offset by as much as 4‰

DOI: 10.1002/hyp

from the theoretical equilibrium condition for waters that flow between open-system environments of contrasting PCO_2. Such settings include groundwater springs and seeps, seepage waters in caves, geothermal waters and headwater catchment streams. Ambiguity as to whether atmospheric CO_2 exchange or outgassing of CO_2 is the cause of high δ^{13}C-DIC values in surface waters can be overcome by determining the excess PCO_2 of the water; isotopic exchange with atmospheric CO_2 is unlikely to be a significant cause of increased δ^{13}C-DIC for waters with PCO_2 values greater than twice that of the surrounding atmosphere. Rather, isotopic fractionation of DIC due to outgassing of CO_2 ought to be considered in future investigations that utilize δ^{13}C-DIC for studying biogeochemical processes in surface waters.

ACKNOWLEDGEMENTS

This work was supported by the Sleepers River Research Watershed, SUNY-ESF and the USGS Watershed, Energy and Biogeochemical Budgets (WEBB) program. Funding for the post-doctoral work of D. H. Doctor was provided by the US National Research Council and the National Research Program of the USGS. D. Choy performed isotopic analysis of water for this study. Reviews by A. White, T. D. Bullen and two anonymous reviewers greatly improved the manuscript.

REFERENCES

Amiotte-Suchet P, Aubert D, Probst JL, Gauthier-Lafaye F, Probst A, Andreux F, Viville D. 1999. δ^{13}C pattern of dissolved inorganic carbon in a small granitic catchment: the Strengbach case study (Vosges mountains, France). *Chemical Geology* **159**: 129–145.

Amundson R, Stern L, Baisden T, Wang Y. 1998. The isotopic composition of soil and soil-respired CO_2: Biogeochemistry of isotopes in soil environments; theory and application. *Geoderma* **82**: 83–114.

Atekwana EA and Krishnamurthy R.V. 1998. Seasonal variations of dissolved inorganic carbon and δ^{13}C of surface waters: application of a modified gas evolution technique. *Journal of Hydrology* **205**(3-4): 265–278.

Aucour A, Sheppard SMF, Guyomar O, Wattelet J. 1999. Use of ^{13}C to trace origin and cycling of inorganic carbon in the Rhône River system. *Chemical Geology* **159**: 87–105.

Billett MF, Storeton-West R, Hargreaves KJ, Flechard C, Fowler D, Palmer SM, Hope D, Deacon C. 2004. Linking land-atmosphere-stream carbon fluxes in a lowland peatland system. *Global Biogeochemical Cycles* **18**: GB1024 1–12.

Bullen TD, Kendall C. 1998. Tracing of weathering reactions and water flowpaths: a multi-isotope approach. In *Isotope Tracers in Catchment Hydrology*, Kendall C, McDonnell JJ (eds). Elsevier: Amsterdam; 611–646.

Cerling TE, Solomon DK, Quade J, Bowman JR. 1991. On the isotopic composition of carbon in soil carbon dioxide. *Geochimica et Cosmochimica Acta* **55**: 3403–3405.

Cole JJ, Caraco NF. 2001. Carbon in catchments: connecting terrestrial carbon losses with aquatic metabolism. *Marine and Freshwater Research* **52**: 101–110.

Cole JJ, Caraco NF, Kling GW, Kratz TK. 1994. Carbon dioxide supersaturation in the surface waters of lakes. *Science* **265**: 1568–1570.

Cosby BJ, Hornberger GM, Galloway JN, Wright RF. 1985. Modelling the effects of acid deposition: assessment of a lumped parameter model of soil water and streamwater chemistry. *Water Resources Research* **21**: 51–63.

Cox PM, Totterdell IJ, Betts RA, Jones CD, Spall SA. 2000. Acceleration of global warming due to carbon-cycle feedbacks in a coupled climate model. *Nature* **408**: 184–187.

Cramer W, Bondeau A, Woodward FI, Prentice IC, Betts RA, Brovkin V, Cox PM, Fisher V, Foley JA, Friend AD, Kucharik C, Lomas MR, Ramankutty N, Sitch S, Smith B, White A, Young-Molling C. 2001. Global response of terrestrial ecosystem structure and function to CO_2 and climate change: results from six dynamic global vegetation models. *Global Change Biology* **7**(4): 357–373.

Davidson GR. 1995. The stable isotopic composition and measurement of carbon in soil CO_2. *Geochimica et Cosmochimica Acta* **59**: 2485–2489.

Deines P, Langmuir D, Harmon RS. 1974. Stable carbon isotope ratios and the existence of a gas phase in the evolution of carbonate ground waters. *Geochimica et Cosmochimica Acta* **38**: 1147–1164.

Epstein S, Mayeda TK. 1953. Variations of ^{18}O of waters from natural sources. *Geochimica et Cosmochimica Acta* **4**: 213–224.

Finlay JC. 2003. Controls of streamwater dissolved inorganic carbon dynamics in a forested watershed. *Biogeochemistry* **62**: 231–252.

Friedlingstein P, Bopp L, Ciais P, Dufresne J-L, Fairhead L, LeTreut H, Monfray P, Orr J. 2001. Positive feedback between future climate change and the carbon cycle. *Geophysical Research Letters* **28**(8): 1543–1546.

Hall LM. 1959. The Geology of the St. Johnsbury Quadrangle, Vermont and New Hampshire. *Vermont Geological Survey Bulletin* no. (13):, 105 p.

Hellings L, Dehairs F, Van Damme S, Baeyens W. 2001. Dissolved Inorganic Carbon in a Highly Polluted Estuary (The Scheldt). *Limnology and Oceanography* **46**(6): 1406–1414.

Hendy CH. 1971. The isotopic geochemistry of speleothems—I. The calculation of the effects of different modes of formation on the isotopic composition of speleothems and their applicability as palaeoclimatic indicators. *Geochimica et Cosmochimica Acta* **35**(8): 801–824.

Hélie J-F, Hillaire-Marcel C, Rondeau B. 2002. Seasonal changes in the sources and fluxes of dissolved inorganic carbon through the St. Lawrence River—isotopic and chemical constraint. *Chemical Geology* **186**: 117–138.

Herczeg AL, Fairbanks RG. 1987. Anomalous carbon isotope fractionation between atmospheric CO_2 and dissolved inorganic carbon induced by intense photosynthesis. *Geochimica et Cosmochimica Acta* **51**(4): 895–899.

Hjerdt KN. 2002. *Deconvoluting the Hydrologic Response of a Small Till Catchment: Spatial Variability of Groundwater Level and Quality in Relation to Streamflow*. Ph.D. thesis, State University of New York, Syracuse, New York, 204 pp.

Hope D, Palmer SM, Billett MF, Dawson JJC. 2001. Carbon dioxide and methane evasion from a temperate peatland stream. *Limnology and Oceanography* **46**: 847–857.

Jones JB, Jr, Mulholland PJ. 1998. Influence of drainage basin topography and elevation on carbon dioxide and methane supersaturation of stream water. *Biogeochemistry* **40**: 57–72.

Jones JB, Jr, Stanley EH, Mulholland PJ. 2003. Long-term decline in carbon dioxide supersaturation in rivers across the contiguous United States. *Geophysical Research Letters* **30**(10): 1–4.

Karim A, Veizer J. 2000. Weathering processes in the Indus River Basin: implications from riverine carbon, sulfur, oxygen, and strontium isotopes. *Chemical Geology* **170**: 153–177.

Kendall C, Mast MA, Rice KC. 1992. Tracing watershed weathering reactions with δ^{13}C. In *Water-Rock Interaction, Proceedings of 7th International Symposium, Park City, Utah*. Kharaka YK, Maest AS (eds). Balkema: Rotterdam; 569–572.

Kendall KA, Shanley JB, McDonnell JJ. 1999. A hydrometric and geochemical approach to test the transmissivity feedback hypothesis during snowmelt. *Journal of Hydrology* **219**(3–4): 188–205.

Kling GW, Kipphut GW, Miller MC. 1991. Arctic lakes and streams as gas conduits to the atmosphere: implications for tundra carbon budgets. *Science* **251**: 298–301.

Kling GW, Kipphut GW, Miller MC. 1992. The flux of CO_2 and CH_4 from lakes and rivers in Arctic Alaska: Toolik Lake. *Hydrobiologia* **240**: 23–36.

Lin G, Ehleringer JR. 1997. Carbon isotopic fractionation does not occur during dark respiration in C3 and C4 plants. *Plant Physiology* **114**(1): 391–394.

Marlier JF, O'Leary MH. 1984. Carbon kinetic isotope effects on the hydration of carbon dioxide and the dehydration of bicarbonate ion. *Journal of the American Chemical Society* **106**: 5054–5057.

Mayorga E, Aufdenkampe AK, Masiello CA, Krusche AV, Hedges JI, Quay PD, Richey JE, Brown TA. 2005. Young organic matter as a source of carbon dioxide outgassing from Amazonian rivers. *Nature* **436**: 538–541.

McGlynn BL, McDonnell JJ, Shanley JB, Kendall C. 1999. Riparian zone flowpath dynamics during snowmelt in a small headwater catchment. *Journal of Hydrology* **222**: 75–92.

Michaelis J, Usdowski E, Menschel G. 1985. Partitioning of ^{13}C and ^{12}C on the degassing of CO_2 and the precipitation of calcite—Rayleigh-type fractionation and a kinetic model. *American Journal of Science* **285**: 318–327.

Mook WG, Bommerson JC, Staverman WH. 1974. Carbon isotope fractionation between dissolved bicarbonate and gaseous carbon dioxide. *Earth and Planetary Science Letters* **22**: 169–176.

Neal C. 1988. Determination of dissolved CO_2 in upland streamwater. *Journal of Hydrology* **99**: 127–142.

Ohte N, Tokuchi N, Suzuki M. 1995. Biogeochemical influences on the determination of water chemistry in a temperate forest basin: factors determining the pH value. *Water Resources Research* **31**(11): 2823–2834.

Palmer SM, Hope D, Billett MF, Dawson JJ, Bryant CL. 2001. Sources of organic and inorganic carbon in a headwater stream: Evidence from carbon isotope studies. *Biogeochemistry* **52**: 321–338.

Park R, Epstein S. 1961. Metabolic fractionation of C^{13} & C^{12} in plants. *Plant Physiology* **36**(2): 133–138.

Pinol J, Avila A. 1992. Streamwater pH, alkalinity, pCO_2 and discharge relationships in some forested Mediterranean catchments. *Journal of Hydrology* **131**: 205–225.

Poage MA, Feng X. 2004. A theoretical analysis of steady state $\delta^{13}C$ profiles of soil organic matter. *Global Biogeochemical Cycles* **18**: GB2016; doi:10·1029/2003GB002195.

Richey JE, Melack JM, Aufdemkampe AK, Ballester VM, Hess LL. 2002. Outgassing from Amazonian rivers and wetlands as a large tropical source of atmospheric CO_2. *Nature* **416**: 617–620.

Rightmire CT. 1978. Seasonal variation in PCO_2 and ^{13}C content of soil atmosphere. *Water Resources Research* **14**: 691–692.

Shanley JB, Chalmers A. 1999. The effect of frozen soil on snowmelt runoff at Sleepers River, Vermont. *Hydrological Processes* **13**: 1843–1857.

Shanley JB, Kendall C, Smith TE, Wolock DM, McDonnell JJ. 2002a. Controls on old and new water contributions to stream flow at some nested catchments in Vermont, USA. *Hydrological Processes* **16**: 589–609.

Shanley JB, Schuster PF, Reddy MM, Roth DA, Taylor HE, Aiken GR. 2002b. Mercury on the move during snowmelt in Vermont. *EOS Trans. AGU* **83**: 45–48.

Shanley JB, Hjerdt KN, McDonnell JJ, Kendall C. 2003. Shallow water table fluctuations in relation to soil penetration resistance. *Ground Water* **41**(7): 964–972.

St Jean G. 2003. Automated quantitative and isotopic (^{13}C) analysis of dissolved inorganic carbon and dissolved organic carbon in continuous-flow using a total organic carbon analyzer. *Rapid Communications in Mass Spectrometry* **17**(5): 419–428.

Stumm W, Morgan JJ. 1981. *Aquatic Chemistry: An Introduction Emphasizing Chemical Equilibria in Natural Waters*, 2nd edition. Wiley Interscience: New York; 780.

Szaran J. 1997. Achievement of carbon isotope equilibrium in the system HCO_3^- (solution)-CO_2(gas). *Chemical Geology* **142**(1–2): 79–86.

Taylor CB, Fox VJ. 1996. An isotopic study of dissolved inorganic carbon in the catchment of the Waimakariri River and deep ground water of the North Canterbury Plains, New Zealand. *Journal of Hydrology* **186**: 161–190.

Telmer K, Veizer J. 1999. Carbon fluxes, pCO_2 and substrate weathering in a large northern river basin, Canada: carbon isotope perspectives. *Chemical Geology* **159**: 61–86.

Usdowski E, Hoefs J. 1990. Kinetic $^{13}C/^{12}C$ and $^{18}O/^{16}O$ effects upon dissolution and outgassing of CO_2 in the system CO_2–H_2O. *Chemical Geology* **80**: 109–118.

Winslow SD, Pepich BV, Bassett MV, Wendelken SC, Munch DJ, Sinclair JL. 2001. Microbial inhibitors for U.S. EPA drinking water methods for the determination of organic compounds. *Environmental Science and Technology* **35**: 4103–4110.

Yang C, Telmer K, Veizer J. 1996. Chemical dynamics of the "St. Lawrence" riverine system: δD_{H2O},$\delta^{18}O_{H2O}$,$\delta^{13}C_{DIC}$,$\delta^{34}S_{sulfate}$, and dissolved $^{87}Sr/^{86}Sr$. *Geochimica et Cosmochimica Acta* **60**(5): 851–866.

Zhang J, Quay PD, Wilbur DO. 1995. Carbon isotope fractionation during gas-water exchange and dissolution of CO_2. *Geochimica et Cosmochimica Acta* **59**: 107–114.